

AIAA 93-3132

**Exploratory Study of Shock Reflection
Near an Expansion Corner**

F.K. Lu and K.-M. Chung

University of Texas at Arlington

Arlington, TX

**AIAA 24th
Fluid Dynamics Conference
July 6-9, 1993 / Orlando, FL**

Exploratory Study of Shock Reflection Near an Expansion Corner

Frank K. Lu* and Kung-Ming Chung†

University of Texas at Arlington, Arlington, Texas 76019-0018

Experiments were performed at Mach 8 in which a shock was reflected off a low Reynolds number, turbulent boundary layer past an expansion corner. The shock was generated by 2- and 4-deg sharp wedges and the corner was either 2.5 or 4.25 deg. The inviscid shock reflection was one boundary layer thickness ahead or behind the corner or at the corner itself. All interactions were unseparated. The dynamic surface pressure distributions were examined together with the case of shock reflection on a flat plate. With shock reflection ahead of the corner, the mean surface pressure downstream was attenuated due to the proximity of the corner. With shock reflection downstream of the corner, the surface pressure distribution showed a reduced upstream influence. The highly swept expansion fan produced a surface pressure which rose gently downstream with no minima, unlike in supersonic flows with the same shock-corner separation distance. In many of the interactions, an anomalous pressure peak was found downstream. The surface pressure through the interaction exhibited unsteadiness. A peak in the rms, 2–3 times that of the incoming rms value, was found ahead of the shock reflection location. Secondary rms peaks were also found downstream.

Nomenclature

M	= Mach number
p	= pressure
s	= distance measured from the inviscid shock reflection location along the test surface, Fig. 1
x	= distance measured from corner along the test surface, Fig. 1
α	= corner angle, Fig. 1
δ	= boundary layer thickness
θ	= external wedge angle, Fig. 1
σ_p	= standard deviation of surface pressure fluctuations
ξ	= pressure ratio across a shock wave or an expansion fan
<i>Subscripts</i>	
<i>incip</i>	= incipient
<i>o</i>	= undisturbed conditions of the boundary layer at the corner location

sh	= shock
U	= upstream influence
w	= mean wall value
1, ..., 4	= inviscid regions, Fig. 1
∞	= incoming freestream or incoming static value

Superscripts
() = normalized by 6,

Introduction

The viscous–inviscid interaction between a shock wave and a turbulent boundary layer remains one of the most interesting and challenging problems of contemporary fluid mechanics. Such an interaction is described as two-dimensional if the mean features do not vary in the direction transverse to the incoming flow. In the supersonic regime, two-dimensional interactions have been well explored experimentally and accurate solutions have been obtained numerically. A recent review of the progress made is given by Ddery and Marvin¹ and a more recent compilation of experimental data can be found in Fernholz et al.² However, there are still significant gaps in understanding the phenomenon. Some of the deficiencies include a lack of adequate knowledge at hypersonic Mach numbers. The unsteadiness existing in a hypersonic shock boundary-layer interaction and the effect of a sequence of disturbances on the boundary layer are also poorly understood.

The motivation of the present study is therefore to further the understanding of shock boundary-layer interactions in the hypersonic regime. An exploration

*Assistant Professor, Aerodynamics Research Center, Mechanical and Aerospace Engineering Department. Senior Member AIAA.

†Graduate Research Associate, Aerodynamics Research Center, Mechanical and Aerospace Engineering Department; presently, Research Associate, Institute of Aeronautics and Astronautics, National Cheng-Kung University, Taiwan, ROC. Student Member AIAA.

Copyright ©1993 by F. K. Lu and K.-M. Chung. Published by the American Institute of Aeronautics and Astronautics, Inc. with permission.

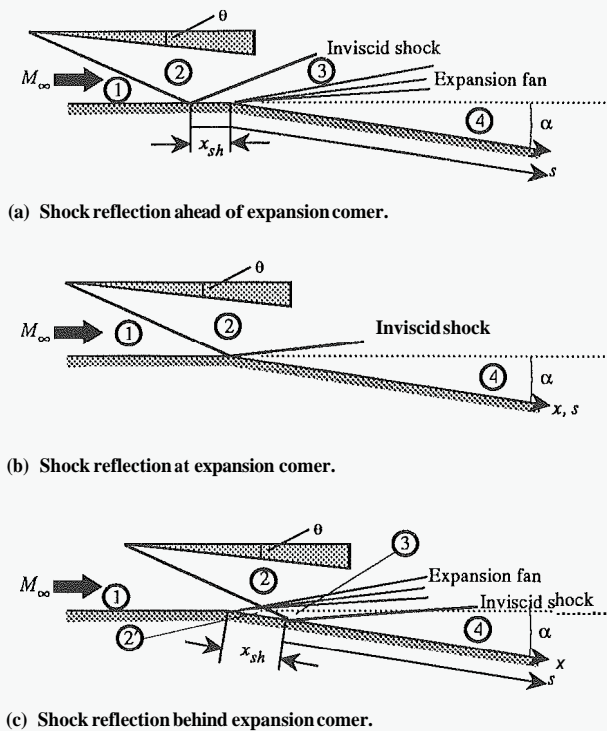


Figure 1: Schematic of test configurations.

of interaction unsteadiness via surface pressure fluctuations is also undertaken. Although the focus of the study is shock reflection near an expansion corner as depicted schematically in Fig. 1, some preceding results concerning shock reflection off a flat surface are also presented. (Fig. 1 includes details that will be described later.)

The combined effect of a shock reflection near an expansion corner, whether ahead or behind, can be regarded as a sequential pressure disturbance upon a turbulent flow. Sequential disturbances represent a complex situation in that the boundary layer is still recovering from the first disturbance when it is subjected to another disturbance. Each disturbance moreover is often comprised of a number of related “effects” acting more or less simultaneously. For example, if the expansion corner in Fig. 1 is absent so that the shock reflects off a flat surface, the boundary layer is subjected to the effects of the shock wave, the subsequent adverse pressure gradient, and an extra strain rate.³

In high-speed flows, sequential multiple disturbances are scarcely understood due to an extreme dearth of studies but are nevertheless commonplace occurrences. Thus Fig. 1a and c idealizes the off-design reflection of a cowl shock at an expansion corner of a jet engine. Some pertinent studies involving multiple pressure disturbances which have come to the authors’

attention include a supersonic study of the geometry depicted in Fig. 1⁴ and the flow past a compression corner followed by an expansion corner.^{5,6} These studies attempt to understand the effects of closely-coupled sequential disturbances on the turbulent boundary layer. In other words, the distance between the sequential disturbances is small so that a non-equilibrium turbulent boundary layer approaches the downstream disturbance. Further, these disturbances are generally such that the succeeding disturbance is opposite and tends to “cancel” the preceding one. (An example of situations where such cancellation does not occur but where the disturbances are of the same type is the multiple shock reflections existing in high-speed duct flows.⁷)

Review of Previous Research

Chew⁴ investigated the configuration shown in Fig. 1 at Mach 2.5 for an adiabatic, turbulent boundary layer in which oblique shocks cause both attached and separated interactions. The inviscid surface pressure distribution consists of step functions and Chew varied the distance between shock reflection and the expansion corner by up to 66. With the corner downstream of the shock, Chew found that the pressure distribution and extent of the separation are strongly modified from the flat plate case. The corner starts to affect the shock-induced interaction when it is 3–46 downstream of the inviscid shock reflection location. The influence of the corner becomes larger as it approaches the shock reflection. Eventually, the corner is able to “neutralize” the reflected shock. With shock reflection downstream of the corner, Chew observed that the mutual influence between the expansion fan and the incident shock ceases at only a small separation distance. Finally, Chew found a complex separation behavior which depends critically on both the presence of the corner and on the incident shock strength.

More recently, Smith and Smits⁶ examined the Mach 3 flow past a 20-deg compression corner followed by a 20-deg expansion corner located about 56, downstream. The compression corner produces a small separated region. The emphasis of this study is on the nonlinear behavior of the mean and turbulent properties. The mean flow near the wall recovers quickly and shows a logarithmic region at 46, downstream of the expansion corner but the mean flow in the outer region recovers more slowly. Further, although turbulent properties near the surface recover quickly, there is no sign that they reach equilibrium at the last measurement station. Within the downstream measurement region, Smith and Smits⁶ found that the skin friction coefficient does not reach the upstream undisturbed level. This was also observed by Zheltovodov et al.⁵ who, moreover, found that in supersonic flows, the interval between the compression and expansion corners strongly affects the recovery process and that this interval effec-

tively becomes smaller if compression causes the flow to separate. This observation is qualitatively similar to Chew's as summarized above.⁴

In the present study, a shock in a Mach 8 flow is reflected at one boundary layer thickness ahead and behind an expansion corner and at the corner itself. This study found a strong "coupling" between the shock and expansion fan, apparently due to the highly swept, hypersonic wave systems embedded within the boundary layer than in a supersonic flow. Even in the unseparated interactions studied, the surface pressure exhibits intermittent behavior and a local rms peak is detected near the upstream influence. Finally, when the shock reflects downstream of the corner, both the mean and unsteady pressure peaks are lower. The interaction size is also smaller. The above features indicate a favorable effect in mitigating the interaction when the shock reflects downstream of the corner.

Experimental Methods

Facility, Models and Test Conditions

The experiments were performed in the University of Texas at Arlington's Hypersonic Shock Tunnel Facility located in the Aerodynamics Research Center.⁸ A brief description of the facility, models, test conditions and experimental methods is now provided; for more details see Ref. 9. By operating the shock tunnel in the "equilibrium interface" mode, high Reynolds number, perfect gas conditions were obtained. To obtain the desired test conditions, the driver tube was charged to 24 MPa \pm 1.5 percent (3,500 psia) while the driven tube was charged to 280 kPa \pm 1.3 percent (40 psia) after first being evacuated to remove moist ambient air. The test section, diffuser, and dump tank were evacuated to below 0.32 kPa (0.05 psia). The gas used throughout the tunnel was dried, unheated air.

The tunnel was started by breaking a pair of diaphragms separating the driver and driven tubes. An unsteady flow was established in these tubes which accelerated the test gas in the driven tube through a 7.5-deg half-angle conical nozzle into an enclosed free-jet test section, 536 mm (21.1 in.) long and 440 mm (17.5 in.) in diameter. The shock that propagated into the driven tube had a Mach number of 2.15 with a run-to-run variation of less than \pm 5 percent. The low shock Mach number ensured that real gas effects were negligibly small. The test conditions for the present study were an incoming freestream velocity of 1.24 km s⁻¹ (4,080 ft/s), a nominal freestream Mach number of 8, stagnation pressure and temperature of 5.38 MPa (780 psia) and 820 K (1,480 °R) respectively and a unit Reynolds number of $Re = 10.2 \times 10^6 \text{ m}^{-1}$ (3.1 million/ft). The static pressure and temperature under the above conditions were 0.55 kPa (0.08 psia) and 59 K (107 °R) respectively and corresponded to conditions

slightly above the air saturation line. The flat plate was at room temperature at about 290 K (522 °R) and thus the experiments were performed under cold-wall conditions.

The three configurations depicted schematically in Figs. 1a–c comprised of a test surface and an external shock generator. The test surface was a sharp-edged flat plate 0.96 m (37.75 in.) long and 0.203 m (8 in.) wide with an expansion corner located at 768 mm (30.25 in.) from the leading edge. The test surface was isolated from the tunnel wall and the lower surface by plates on both of its sides. Due to the limited length of the test section, the flat plate protruded into the nozzle and diffuser. Consequently, the boundary layer developing over the flat plate was initially subjected to a favorable pressure gradient. The surface pressure in the test region however showed only an extremely slight, favorable longitudinal pressure gradient which can be safely ignored. A nominally two-dimensional, turbulent boundary layer with thickness $\delta = 12 \pm 2 \text{ mm}$ ($0.47 \pm 0.08 \text{ in.}$) developed naturally ahead of the test region. The Reynolds number based on the momentum thickness of the undisturbed boundary layer was $Re_\theta = 1800\text{--}2300$ and therefore the boundary layer showed characteristics typical of low Reynolds number flow such as the lack of a wake component. A more detailed description of the boundary layer can be found in Refs. 10 and 11. The useful "quasi-steady" test time was about 0.5 ms and this provided a slug of test gas about 0.6 m (2 ft) long. The interaction region around the corner was about 0.2 m (0.7 ft) or one-third the length of test gas and this length more than fulfilled the requirement for a fully-developed turbulent flow to exist.¹¹

Two different expansion-corner inserts with convex angles $\alpha = 2.5$ and 4.25 deg were used for the experiments. Although these angles appeared small, they produced significant inviscid pressure drops comparable to much larger supersonic corners. A shock was reflected near the expansion corner by an external shock generator attached to an angle-of-attack adapter. The shock generator was 133 mm (5.25 in.) long, 178 mm (7.0 in.) wide and 12.7 mm (0.5 in.) thick. The leading-edge bevel was 25 deg. Due to the lack of previous studies of shock impingement near an expansion corner, it was thought that a systematic approach would be to study weak, unseparated interactions first. Two adapters that set the angle of attack of the shock generator to $\theta = 2$ and 4 ± 0.1 deg were used to mount the shock generator to a sting. The shock generator was located with its tip 76 mm (3 in.) above the test surface such that an inviscid shock was reflected off the test surface at $\bar{x}_{sh} \square x_{sh}/\delta_o = \{-1, 0, 1\}$ from the corner. The unseparated interactions due to shock reflection were not expected to suffer from three-dimensional effects." This is especially the case at high Mach number in which the Mach cones from the tips of the shock generator are ex-

tremely slender compared to lower Mach numbers.

In Fig. 1, the inviscid regions of interest are labeled by 1–4. The distance along the test surface measured from the corner is x while the distance along the test surface measured from the inviscid shock reflection is s . The two coordinates s and x facilitate the discussion since two different viewpoints can be adopted for understanding the interaction — the first is that of the shock affecting the corner flow while the second is vice versa. Fig. 1b shows a shock reflected at the expansion corner. This situation arises when $\theta > \alpha$; otherwise, the reflection consists of an expansion fan while the shock is cancelled if $\theta = \alpha$. Not shown in Figs. 1a–c is the case of shock reflection off a flat surface which is pertinent to the present study. This case can be considered as shock deflection off a zero-deg corner. For consistency, the inviscid regions are denoted 1, 2 and 4, as in Fig. 1b. In the studies, the incident shock strength was $\xi_{21} \equiv p_2/p_1 = 1.47$ and 2.09, whereas the overall pressure ratio used as a measure of interaction strength ranged from $\xi_{41} \equiv p_4/p_1 = 0.95$ –4.05, with the strongest interaction occurring with shock reflection off a flat surface. In all cases, unseparated interactions were induced based on previous investigations.’ In addition, there was a case where $\xi_{41} \approx 1$ generated by $(\alpha, \theta) = (4.25^\circ, 2^\circ)$ in which the nonlinear nature of the inviscid shock-expansion process is evident. For comparison, in Chew’s experiments at Mach 2.5,⁴ $\xi_{21} = 1.3$ –1.66 and $\xi_{41} = 1.14$ –2.61, with separation occurring at the highest interaction strength when $\theta = 8$ deg.

Measurement Techniques

The diagnostics comprised surface pressure measurements across the corner centerline from 38.1 mm (1.5 in.) upstream to 60.3 mm (2.375 in.) downstream spaced 6.35 mm (0.25 in. or 0.476,) apart. Kulite Models XCS-093-5A (0–35 kPa, 0–5 psia) and XCS-093-50A (0–350 kPa, 0–50 psia) pressure transducers with sensing surfaces of 0.97 mm (0.038 in.) diameter and protective screens of 0.97 mm (0.038 in.) diameter were potted in place using silicone rubber sealant and were flushed perpendicularly with the test surface to better than $\pm 0.005\delta_0$. Natural frequencies of the transducers were quoted by the manufacturer as 100 kHz and 275 kHz respectively. The transducer signals were conditioned by instrumentation amplifier–filters with a bandwidth of up to 100 kHz. Eight high-speed digitizers were used to acquire data simultaneously at a rate of one million samples per second per channel. The data were stored in a 286-type host computer for later reduction and analyses. In post-processing, digital filtering was used to set the upper frequency of the signals to 100 kHz, which also removed high-frequency transducer noise and which gave a signal-to-noise ratio of 10:1 for low pressures to 20:1 for higher pressures.

A static calibration sufficed for determining the transducer sensitivities even though the transducers were used in dynamic situations.¹³ The drift and hysteresis of these transducers were significant, especially if the transducers were used to measure low pressures. To reduce drift, the transducers were calibrated during evacuation of the test section against an MKS Baratron Model 127A vacuum gauge, a capacitance-type manometer accurate to ± 7 Pa (f0.001 psia) that is used widely as a secondary standard. The transducers’ sensitivities were obtained by linear least-squares fits to the Calibration data. Significant zero shift occurred in the thirty minutes that elapsed between a run and the preceding calibration. The shift problem was overcome by “renulling” the transducers through comparing their outputs against the vacuum gauge prior to tunnel firing. Subsequently, the acquired data were converted into engineering units, with the sensitivities obtained from calibration and the offsets obtained from the final renulling adjustment. The calibrations were checked continually throughout the daily test sequence and the transducers were re-calibrated if necessary. Other problems of piezoresistive transducers, namely, thermal zero shift and thermal sensitivity were negligible due to the short run times of the tests.

The limited number of data acquisition channels meant that detailed surface pressure distributions were obtained with a number of runs. Seven channels were used to measure interaction surface pressures while the eighth was used to measure a reference pressure p_∞ 34.9 mm (1.375 in. or 2.66,) ahead of the corner. The measured interaction pressures were normalized by p_∞ to minimize the effects of run-to-run variations. Unused orifices were plugged with dummy transducer replicas made from steel rods.

The high-speed data acquisition system allowed an exploration of the surface pressure fluctuations to be attempted. The bandwidth of the data was about 2–100 kHz, the lower cutoff frequency being determined by the available test time of about 0.5 ins, and about 60 percent of the rms fluctuations were captured within the data bandwidth.^{11,14} Such unsteady data are always plagued by their limited bandwidth, a problem exacerbated at high speeds due to the extremely broad spectra of the signals. The inability to resolve the highest frequencies means that knowledge on the spectral behavior of the finest scales is missing. In the present experiments, about 500 data points per record were obtained and these data were deemed adequate for statistical analyses within the constraints of the limited data bandwidth. As a check of the validity of the above statement, a number of data records were divided into two halves and the mean and rms values of these halves were compared. The mean and rms values of the two halves differed from one to twelve percent and on average they differed by six percent. Therefore, it was thought that the amount of data per record was suffi-

cient.

The previously mentioned bandwidth limitation can be understood by considering the frequency and spatial resolutions of the transducers. The 100-kHz data bandwidth yielded an upper nondimensional frequency $f\delta/U_\infty$ of about unity which is low compared to previous supersonic experiment¹⁵. The frequency resolution was also compared with those of different investigations by using a reduced frequency $f\nu_w/U_\tau^2$ which in the present experiments was approximately 0.008. This is also comparatively low.¹⁵ In addition to the bandwidth limitation, high frequency damping was also partly due to limited spatial resolution. The nondimensional transducer diameter $d^+ \equiv U_\tau d/\nu_w$, where d is the transducer diameter, was approximately 200 and was in the 50–500 range of most supersonic experiments.¹⁵ At present, it is not clear how $f\delta/U_\infty$, $f\nu_w/U_\tau^2$ or d^+ can be used to provide proper estimates of transducer spatial and frequency resolutions at high Mach numbers. Finally, no corrections were made to the data due to the transducer size.

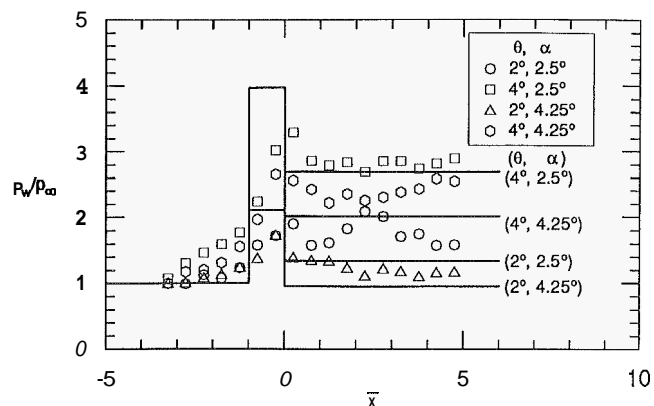
Results and Discussion

Mean Surface Pressure Characteristics

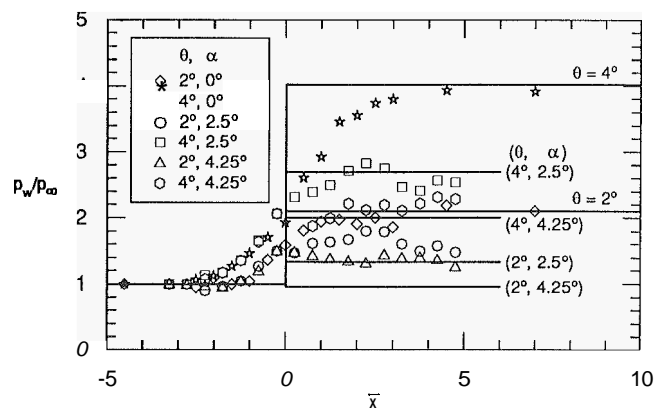
The mean surface pressure distribution is shown in Fig. 2 for $\bar{x}_{sh} = \{-1, 0, 1\}$. Fig. 2b also includes the distribution for shock reflection off a flat plate, namely, with $\alpha = 0$ deg. The inviscid pressure distribution is shown as solid lines in the figures. In all the cases studied, the interaction is unseparated because the surface pressure distribution does not exhibit a kink or a dip. Moreover, based on previous flat-plate results,¹⁵ the present interactions are also expected to be unseparated.

The measured surface pressure starts to rise ahead of the inviscid shock reflection location and the onset of the pressure rise is known as the upstream influence of the shock. With shock reflection ahead of the corner, Fig. 2a shows that the surface pressure is prevented by the expansion corner from rising to the inviscid pressure level behind the reflected shock p_3 . The reason for such a behavior is that, in the absence of the corner, the pressure recovers to the downstream inviscid value in a distance of $x \approx 1.2$ and 4.6 respectively for the $\theta = 2$ deg and 4 deg cases; this can be deduced from Fig. 2b for shock reflection off a flat plate. With shock reflection at $\bar{x}_{sh} = -1$, however, the expansion corner is too close to preclude pressure recovery. Thus, the pressure does not fully recover to the downstream shock value but drops due to the influence of the expansion. Moreover, although the pressure eventually reaches the approximate downstream inviscid value, anomalous pressure peaks can be observed. These will be discussed later.

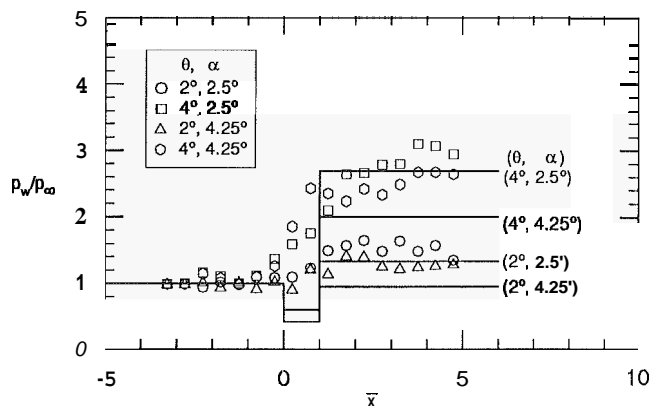
When the shock is reflected at the expansion corner, the inviscid pressure exhibits a step distribution. Simi-



a. Shock ahead of expansion corner.



b. Shock on expansion corner and on flat plate.



c. Shock behind of expansion corner.

Figure 2: Surface pressure distributions.

lar to shock reflection off a flat plate, the present shock reflection at the expansion corner produces a monotonically increasing pressure distribution whereby the interaction extent decreases with a decrease in overall interaction strength ξ_{41} . However, for the case of shock cancellation, with $\theta = 2$ deg and $\alpha = 4.25$ deg, the downstream pressure is higher than the inviscid value and it is not possible at this stage to provide conclusive explanations on this. One explanation is a misalignment of the shock generator since a small change in its angle can contribute to a measurable difference in surface pressure downstream. Furthermore, in Fig. 2b, the downstream inviscid pressures due to a shock induced by a 2-deg generator and that due to a shock induced by a 4-deg generator reflecting off a 4.25-deg expansion corner are about the same. It is interesting to note that the actual interaction pressure distribution for these two cases are close to one another. Thus, it seems plausible that for shock reflection at an expansion corner, the interaction is governed by the overall strength ξ_{41} .

When the shock is reflected downstream of the corner, the surface pressure is significantly affected by the corner. For example, unlike supersonic flows,⁴ the surface pressure in the present experiments does not reach the inviscid pressure “valley” $\xi_{2'1} = p_{2'}/p_1$. This is indicative of a more uniform pressure distribution and a longer distance required by the flow to reach the downstream pressure level in a hypersonic flow.¹⁷ A strong coupling exists between the upstream expansion fan and the downstream shock, with these wave systems substantially embedded through the boundary layer due to their shallow inclinations. Just as in the shock-ahead interaction where the expansion corner prevents the pressure from reaching p_2/p_1 , analogously, in the corner-ahead interaction, the shock prevents the pressure from reaching $p_{2'}/p_1$.

Moreover, in almost all the cases studied, whether the inviscid shock is ahead, at, or behind the corner, an anomalous behavior is observed in that the downstream surface pressure appears to peak at a value higher than that of inviscid flow. The surface pressure peak is especially pronounced at $\bar{x} = 2-3$ for the weakest shock-expansion interactions. No peak is evident in shock reflection off a flat surface, however, see Fig. 2b. This “overshoot” phenomenon differentiates the unseparated interaction from that of unseparated shock reflection on a flat plate and is more akin to that found in the separated interaction arising from shock reflection off a flat plate. The “overshoot” is also observed by Chew⁴ whose measurements further downstream showed that the pressure eventually recovers to the downstream inviscid value. Chew attributed the overshoot to three-dimensional effects although, as discussed previously, these are negligible in the present unseparated interactions. Further, unlike Chew’s experiments, the present downstream pressure tends to

be higher than the inviscid level. In Chew’s data, the surface pressure drops from a peak to below the inviscid level and then rises gently to nearly the inviscid value at $\bar{x} \gtrsim 12$, further downstream than the present measurements can achieve. Chew attributes the pressure drop to mixing losses associated with the large “interaction scales.”

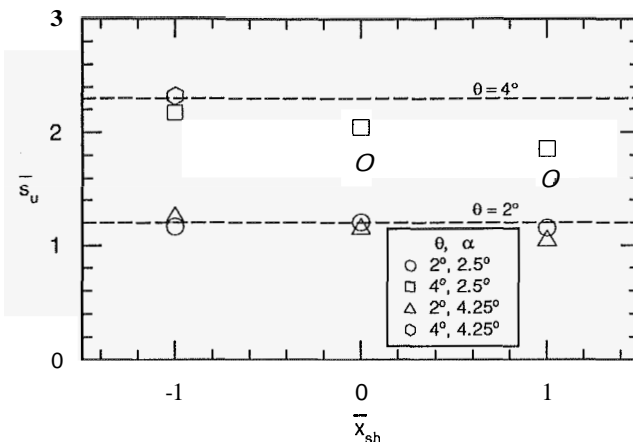


Figure 3: Upstream influence due to shock reflection near expansion corners.

From the mean surface pressure distribution, a normalized upstream influence of the shock $\bar{s}_u = s_u/\delta_o$ can be estimated as the maximum tangent to the upstream pressure distribution with the incoming pressure level” to an accuracy of ± 0.2 . When the shock is reflected behind the corner, the upstream influence is more difficult to estimate, especially for the weaker interactions induced by the 2-deg shock generator, Fig. 2c. However, the upstream influence appears to be reduced. This behavior is also found by Chew⁴ in supersonic interactions. He moreover found that the upstream influence increases with a further movement of the shock downstream, indicating that the expansion corner is exerting less of an influence on the interaction. Apparently, the proximity of the expansion corner produces a favorable pressure gradient which “obstructs” upstream propagation arising from the shock boundary-layer interaction. The above observations of the upstream influence are summarized in Fig. 3. It can be seen that the stronger shock produces a larger upstream influence. In addition, this plot shows that at a particular shock reflection location, the upstream influence is increased when the expansion corner angle is reduced. Consequently, it is postulated that the case of shock reflection off a flat plate sets the upper limit to the upstream influence. The upstream influence for shock reflection on a flat plate is extracted from Fig. 2b and is indicated in Fig. 3 by dashed horizontal lines.

The presence of an expansion corner ahead of an

impinging shock can be thought of as modifying the incoming boundary-layer characteristics. Thus, the upstream pressure propagation at incipient separation depends on the incoming freestream Mach number and on the Reynolds number based on wall conditions $Re_w = U_\tau \delta / \nu_w$.¹⁶ Elfstrom found that for incipient separation, the upstream influence decreases with an increase in Re_w , and it appears plausible that this behavior may be expected to hold for attached interactions as well. For small expansion corners in hypersonic, high Reynolds number flow, the friction velocity and the dynamic viscosity at the wall do not differ greatly from incoming values.¹⁹ However, the expansion produces a thickening of the boundary layer⁹ and thereby an increase in Re_w . Consequently, a decrease in the upstream influence is expected.

Surface Pressure Unsteadiness

In the present unseparated interactions, the surface pressure distribution exhibits unsteadiness which, according to Laganelli et al.,²⁰ is due to an increase in static pressure. The presence of increased unsteadiness is shown in Figs. 4 and 5. In these figures, the ordinate $\sigma_p / \sigma_{p,o}$ is the rms of the pressure fluctuations normalized by the incoming value. Such a plot allows the increase or decrease in the rms value to be compared against the incoming, flat plate value. (For reference, the rms surface pressure of the undisturbed boundary layer is about 8 percent of the mean surface pressure.) The above choice in normalizing the rms pressure is thought to be more meaningful than normalizing the rms pressure by either the local static pressure or the incoming dynamic pressure;²¹ such plots are available in Ref. 9.

With shock reflection ahead of the corner, the normalized pressure fluctuation increases sharply to a peak at the vicinity of the upstream influence. The peak rms is thought to be associated with a strong intermittent behavior of the interaction arising from shock oscillations. These shock oscillations are generally associated with separated interactions at supersonic Mach numbers²² but has not been widely observed at hypersonic Mach numbers. (However, an example of heat flux fluctuations in the unseparated supersonic, shock-reflection interaction was reported by Hayashi et al.²³) These peaks are about two to three times the incoming rms value²⁰ when the shock reflects ahead of the weaker corner. However, the stronger corner attenuates the peak somewhat and therefore appears to affect the unsteadiness more than the mean. Another rms pressure peak is found at the vicinity of the corner. This rms peak is not distinctly seen in shock reflection at an expansion corner or off a flat plate.⁹ Further downstream, the rms pressure decreases due to damping by the expansion corner⁹ before rising again later. This downstream increase in surface pressure fluctuations may be

due to a change in the boundary layer state, from one that is “relaminarizing” due to the favorable pressure gradient to one that is “retransitioning” as the boundary layer redevelops to a new equilibrium state. Also, the downstream peak in the surface pressure fluctuations coincides with the downstream peak in the mean surface pressure at $\bar{x} \approx 2-3$. Similar features are found in cases of shock reflection off and behind an expansion corner and will not be elaborated further.

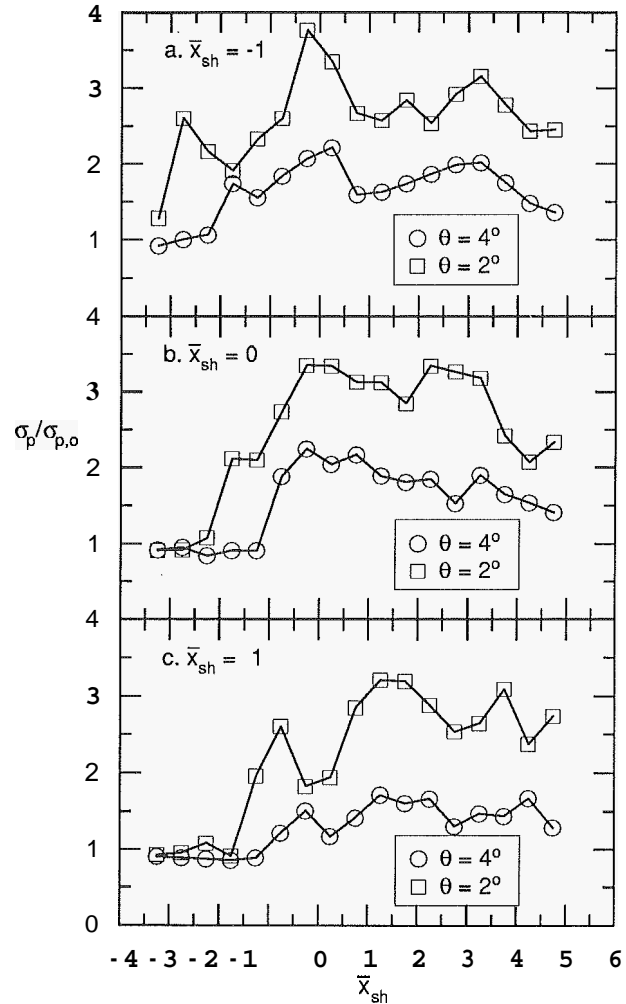


Figure 4: Root-mean-square surface pressure distribution due to shock reflection near the 2.5-deg expansion corner.

Conclusions

An experimental study at Mach 8 of the unseparated interaction arising from shock reflection near an expansion corner shows that the expansion corner exerts a complicated influence on the shock boundary-layer interaction. A strong coupling exists between the shock and the expansion fan within the boundary layer due to the highly swept nature of these wave systems. When the shock is reflected ahead of the corner, the close proximity of the corner prevents the pressure to rise to the downstream inviscid shock value. When the shock is reflected behind the corner, the upstream influence is decreased. However, in the on-corner interaction, the mean surface pressure rises in a non-monotonic way as in shock reflection off a flat plate. Intermittent behavior is found to exist in the surface pressure. For the case of inviscid wave cancellation, the rms surface pressure downstream remains within the level encountered ahead of the interaction. Finally, the reduced interaction length scale and surface pressure unsteadiness when the shock reflects downstream of the corner are indications of a favorable interference effect of the expansion.

Acknowledgements

The research was supported by NASA Langley Research Center through Grant No. NAG 1-891 monitored by Dr. John P. Weidner. This support is gratefully acknowledged. We thank Jim Holland and Gene Sloan for fabricating the models and for ensuring smooth operation of the shock tunnel.

References

1. Déleré, J. and Marvin, J. G., "Shock-Wave Boundary Layer Interactions," AGARD-AG-280, 1986.
2. Fernholz, H. H., Finley, P. J., Dussauge, J. P. and Smits, A. J., "A Survey of Measurements and Measuring Techniques in Rapidly Distorted Compressible Turbulent Boundary Layers," AGARD-AG-315, 1989.
3. Smits, A. J. and Wood, D. II., "The Response of Turbulent Boundary Layers to Sudden Perturbations," *Annual Review of Fluid Mechanics*, Vol. 17, 1985, pp. 321-358.
4. Chew, Y. T., "Shockwave and Boundary Layer Interaction in the Presence of an Expansion Corner," *Aeronautical Quarterly*, Vol. XXX, 1979, pp. 506-527.
5. Zheltovodov, A. A., Shilein, E. H. and Yakovlev, V. N., "Evolution of Turbulent Boundary Layer

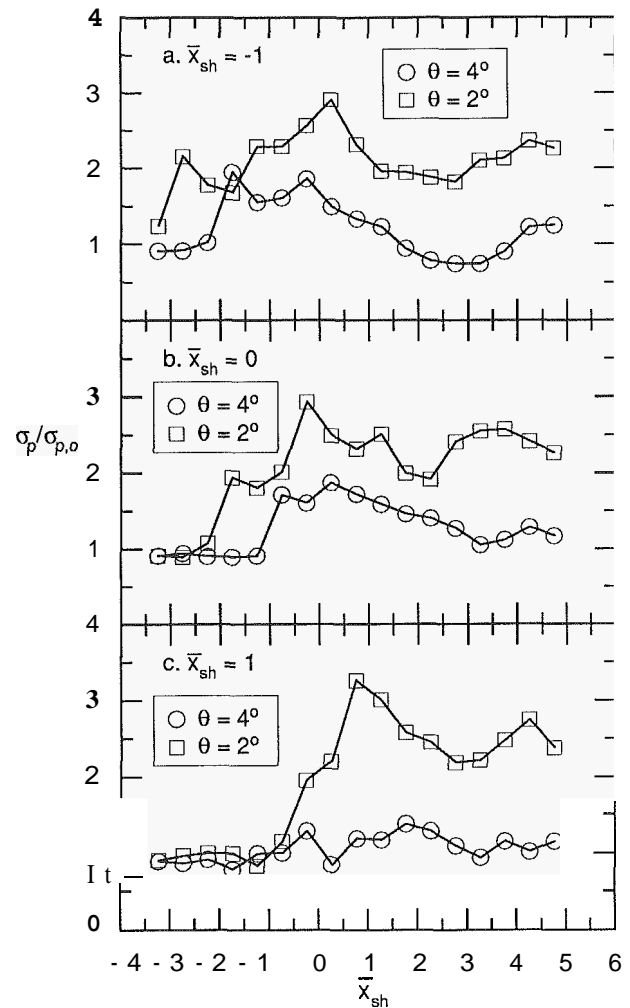


Figure 5: Root-mean-square surface pressure distribution due to shock reflection near the 4.25-deg expansion corner.

- at Conditions of Mixed Interaction with Shock and Expansion Waves,” Preprint No. 12-82, USSR Academy of Sciences, Institute of Theoretical and Applied Mechanics, Novosibirsk, Russia, 1983.
6. Smith, D. R. and Smits, A. J., “The Effect of Successive Distortions on the Boundary Layer in a Supersonic Flow,” AIAA Paper 92-0309, January 1992.
 7. Carroll, B. F. and Dutton, J. C., “Characteristics of Multiple Shock Wave/Turbulent Boundary-Layer Interactions in Rectangular Ducts,” *Journal of Propulsion and Power*, Vol. 6, No. 2, 1990, pp. 186–193.
 8. Lu, F. IC., “Initial Operation of the UTA Shock Tunnel,” AIAA Paper 92-0331, January 1992.
 9. Chung, K.-M., “Shock Impingement Near Mild Hypersonic Expansion Corners,” Ph.D. Dissertation, University of Texas at Arlington, December 1992.
 10. Chung, K.-M. and Lu, F. IC., “An Experimental Study of a Cold-Wall Hypersonic Boundary Layer,” AIAA Paper 92-0312, January 1992.
 11. Chung, K.-M. and Lu, F. K., “Damping of Surface Pressure Fluctuations in Hypersonic Turbulent Flow Past Expansion Corners,” *AIAA Journal*, to be published, 1993.
 12. Reda, D. C. and Murphy, J. D., “Sidewall Boundary-Layer Influence on Shock Wave/Turbulent Boundary-Layer Interactions,” *AIAA Journal*, Vol. 11, No. 10, 1973, pp. 1367–1368.
 13. Chung, K.-M. and Lu, F. IC., “Shock-Tube Calibration of a Fast-Response Pressure Transducer,” AIAA Paper 90-1399, June 1990.
 14. Schewe, G., “On the Structure and Resolution of Wall-Pressure Fluctuations Associated with Turbulent Boundary-Layer Flows,” *Journal of Fluid Mechanics*, Vol. 134, 1983, pp. 311–328.
 15. Dolling, D. S. and Dussauge, J. P., “Fluctuating Wall-Pressure Measurements,” Chapter 8 of Ref. 2, 1989.
 16. Elfstroin, G. M., “Turbulent Hypersonic Flow at a Wedge-Compression Corner,” *Journal of Fluid Mechanics*, Vol. 53, 1972, pp. 113–127.
 17. Lu, F. IC. and Chung, K.-M., “Downstream Influence Scaling of Turbulent Flow Past Expansion Corners,” *AIAA Journal*, Vol. 30, No. 12, 1993, pp. 2976–2977.
 18. Settles, G. S. and Bogdonoff, S. M., “Scaling of Two- and Three-Dimensional Shock/Boundary-Layer Interactions at Compression Corners,” *AIAA Journal*, Vol. 20, No. 6, 1983, pp. 782–789.
 19. Adamson, T. C., “Effect of Transport Properties on Supersonic Expansion Around a Corner,” *Physics of Fluids*, Vol. 10, No. 3, 1967, pp. 953–962.
 20. Laganelli, A. L., Wolfe, H. W. and Wentz, IC R., “Prediction of Fluctuating Pressure in Attached and Separated Compressible Flow,” AIAA Paper 93-0286, January 1993.
 21. Laganelli, A. L., Martellucci, A. and Shaw, L. L., “Wall Pressure Fluctuations in Attached Boundary-Layer Flow,” *AIAA Journal*, Vol. 21, No. 4, 1983, pp. 495–502.
 22. Dolling, D. S., “Fluctuating Loads in Shock Wave/Turbulent Boundary Layer Interactions—Tutorial and Update,” AIAA Paper 93-0284, January 1993.
 23. Hayashi, M., Aso, S. and Tan, A., “Unsteady Aerodynamic Heating Phenomena in the Interaction of Shock Wave/Turbulent Boundary Layer,” *Memoirs of the Faculty of Engineering, Kyushu University*, Vol. 47, No. 4, 1987, pp. 231–239.